

Analysis of β ray spectroscopy

PH3105

2024-11-15

Debayan Sarkar
22MS002

Diptanuj Sarkar
22MS038

Sabarno Saha
22MS037



Contents

I. Introduction	1
II. Theory	1
II.1. β ray spectrometer	1
II.2. Decay Scheme of $^{22}_{11}\text{Na}$ and $^{90}_{38}\text{Sr}$	1
II.2.A. β decay	1
II.2.B. Decay scheme for $^{22}_{11}\text{Na}$	2
II.2.C. Decay scheme for $^{90}_{38}\text{Sr}$	2
II.3. Kinetic Energy of β Particles	3
III. Results and Analysis	4
III.1. $^{22}_{11}\text{Na}$ Source	4
III.1.A. Table for $^{22}_{11}\text{Na}$ Source	4
III.1.B. Plot of Energy vs Count for $^{22}_{11}\text{Na}$ Source	4
III.1.C. Energy corresponding to the maximum count for $^{22}_{11}\text{Na}$ source	5
III.2. $^{90}_{38}\text{Sr}$ Source	5
III.2.A. Table for $^{90}_{38}\text{Sr}$ Source	5
III.2.B. Plot of Energy vs Count for $^{90}_{38}\text{Sr}$ Source	7
III.2.C. Energy corresponding to the maximum count for $^{90}_{38}\text{Sr}$ source	8
IV. Sources of Error	8
V. Conclusion	8

I. Introduction

In this experiment, we perform β ray spectroscopy using a GM Counter. We measure the energy of the β particles emitted by $^{22}_{11}\text{Na}$ and $^{90}_{38}\text{Sr}$. We use this with a Hall probe to measure the energy of the β particles.

II. Theory

We lay out, in brief, the theory behind the β ray spectrometer used, and the decay of the radioactive sources that produce the β rays in our interaction.

II.1. β ray spectrometer

β -spectrometer theory goes here.

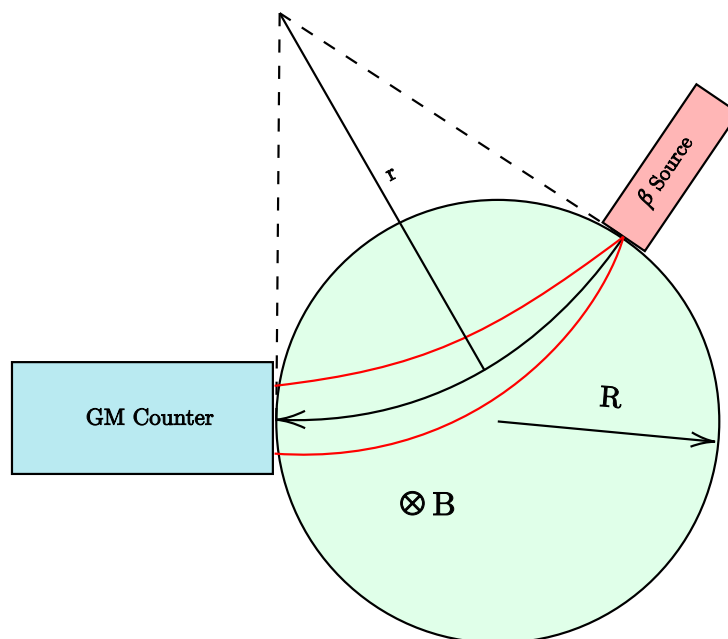


Figure 1 :: lolcat

II.2. Decay Scheme of $^{22}_{11}\text{Na}$ and $^{90}_{38}\text{Sr}$

We will detail out the β decay process and then We detail the β ray decay scheme of the $^{22}_{11}\text{Na}$ and $^{90}_{38}\text{Sr}$, both of which we will use in the experiment.

II.2.A. β decay

The β decay is a type of radioactive decay in which a beta particle is emitted. There are three types of beta decay processes: beta-minus decay, beta-plus decay or electron capture.

1. β^- decay : In beta-minus decay, a neutron decays into a proton, an electron, and an electron antineutrino.

$$n \longrightarrow p^+ + e^- + \bar{\nu}_e \quad [1]$$

2. β^+ decay : In beta-plus decay, a proton decays into a neutron, a positron, and an electron neutrino.

$$p^+ \longrightarrow +e^+ + \nu_e \quad [2]$$

3. **Electron Capture** : In electron capture, an electron is captured by a proton in the nucleus, transforming it into a neutron and emitting a neutrino.

$$p^+ + e^- \longrightarrow n + \nu_e \quad [3]$$

II.2.B. Decay scheme for $^{22}_{11}\text{Na}$

$^{22}_{11}\text{Na}$ undergoes a beta decay(β_+ emission) to form $^{22}_{10}\text{Ne}$ with an intermediate $^{22}_{10}\text{Ne}$ excited state. The excited state of $^{22}_{10}\text{Ne}$ then decays to the ground state by emitting a gamma ray. This is one the of the three decay processes that take place. The other two are the electron capture and the gamma decay to the stable $^{22}_{10}\text{Ne}$. The gamma decay to $^{22}_{10}\text{Ne}$ occurs with negligible probability so we can ignore that. Here we consider the beta decay and the electron capture.

$$(\beta + \text{decay})^{22}_{11}\text{Na} \longrightarrow ^{22}_{10}\text{Ne}^* + e^+ + \nu_e \quad (EC)^{22}_{11}\text{Na} \longrightarrow ^{22}_{10}\text{Ne}^* + \nu_e \quad [4]$$

The decay scheme for $^{22}_{11}\text{Na}$ is shown below.

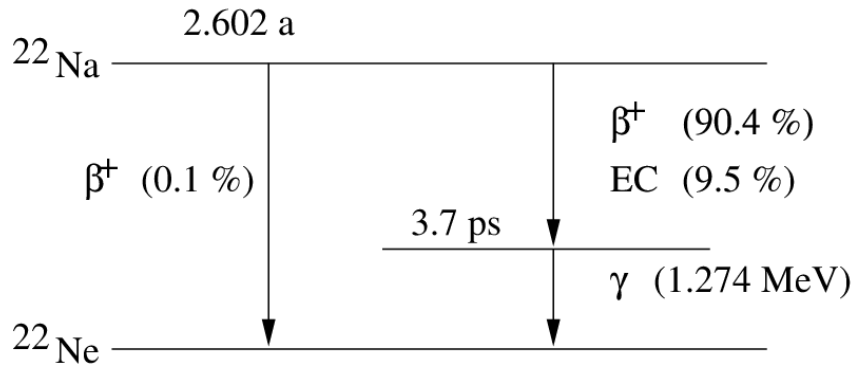


Figure 2 :: Decay scheme for $^{22}_{11}\text{Na}$, Source: Internet

II.2.C. Decay scheme for $^{90}_{38}\text{Sr}$

$^{90}_{38}\text{Sr}$ decays to form $^{90}_{40}\text{Zr}$ by beta decay(β_- emission) with an intermediate daughter nucleus $^{90}_{30}\text{Y}$. There are other decay processes. $^{90}_{30}\text{Y}$ can decay into an intermediate excited state of $^{90}_{40}\text{Zr}^*$. The decay scheme for $^{90}_{38}\text{Sr}$ is shown below.

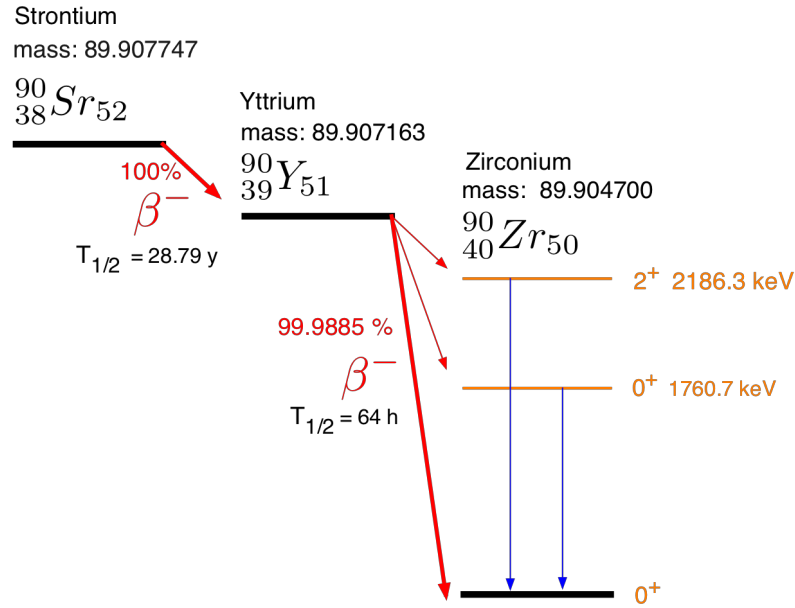
$$(\beta - \text{decay})^{90}_{38}\text{Sr} \longrightarrow ^{90}_{30}\text{Y} + e^- + \bar{\nu}_e \quad [5]$$

and then $^{90}_{30}\text{Y}$ decays to $^{90}_{40}\text{Zr}^*$ by beta decay ox

$$^{90}_{30}\text{Y} \longrightarrow ^{90}_{40}\text{Zr}^* + e^- + \nu_e \longrightarrow ^{90}_{40}\text{Zr} + e^- + \bar{\nu}_e + \gamma \quad (\text{Decay Scheme 1}) \quad [6]$$

or directly having a β decay to $^{90}_{40}\text{Zr}$.

$$^{90}_{30}\text{Y} \longrightarrow ^{90}_{40}\text{Zr} + e^- + \bar{\nu}_e \quad (\text{Decay Scheme 2}) \quad [7]$$

Figure 3 :: Decay scheme for $^{90}_{38}\text{Sr}$, Source: Internet

II.3. Kinetic Energy of β Particles

We use a Geiger-Muller counter to measure the energy of the gamma-ray emitted by the sources. Now, GM counters are not designed to measure energy since, in the Geiger Muller region of the characteristics curve, all energy information is lost. The spectrometer schema is laid out above. We find the relation between the counts and the energy of the beta-ray. Let us now derive the energy of the beta ray. The relativistic energy equation is given by:

$$E = \sqrt{p^2 c^2 + m_0 c^4} \quad [8]$$

where p is the momentum of the beta particle, m_0 is the rest mass of the beta particle, E is the total energy of the beta particle and c is the speed of light.

We also have $E = T + V = T + m_0 c^2$. Using this, we can write the above equation as:

$$T = \sqrt{p^2 c^2 + m_0 c^4} - m_0 c^2 \quad [9]$$

We place the beta source in a magnetic field and use the value for the average radius of curvature r to equate the Lorentz force with the centripetal force (mv^2/r). This gives us:

$$\frac{mv^2}{r} = q(E + vB) = qvB \Rightarrow p = mv = qBr \quad [10]$$

where q is the charge of the beta particle. Using this in the above equation, we get:

$$T = \sqrt{(qBr)^2 + m_0 c^4} - m_0 c^2 \quad [11]$$

III. Results and Analysis

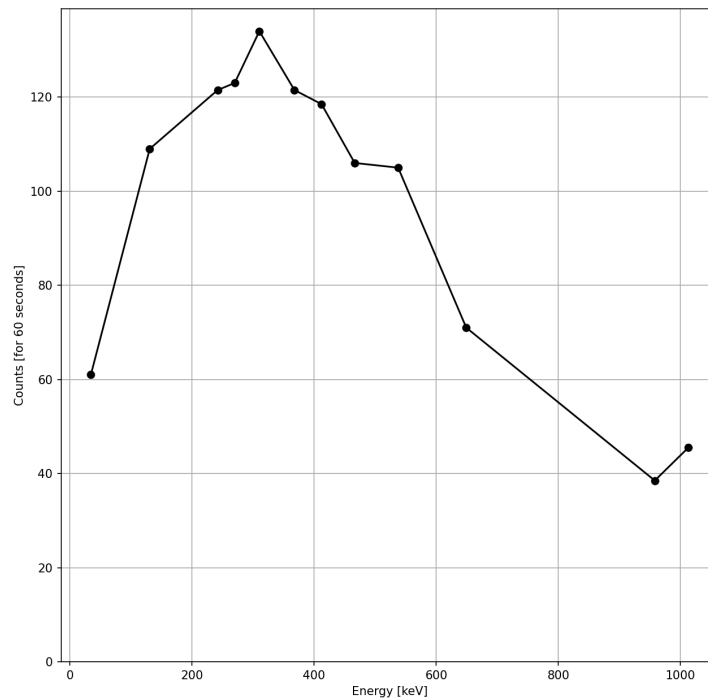
III.1. $^{22}_{11}\text{Na}$ Source

For the $^{22}_{11}\text{Na}$ source, for each voltage we took 2 runs, for 60 seconds each. The energy was calculated using the formula derived above, in kilo electron volts.

III.1.A. Table for $^{22}_{11}\text{Na}$ Source

Magnetic Field(mT)	Voltage (V)	Current (A)	Counts(Run 1)	Counts(Run 2)	Avg. Counts	Energy (keV)
12.7	0.13	0.3	59	63	61	3.43E+01
25.9	0.26	0.6	116	102	109	1.31E+02
36.9	0.38	0.9	121	122	121	2.42E+02
39.4	0.41	1	125	121	123	2.70E+02
42.9	0.45	1.1	138	130	134	3.11E+02
47.7	0.5	1.2	113	130	121	3.68E+02
51.3	0.54	1.3	114	123	118	4.12E+02
55.6	0.58	1.4	108	104	106	4.67E+02
61.1	0.64	1.5	117	93	105	5.38E+02
69.5	0.74	1.8	66	76	71	6.50E+02
91.9	0.9	2.1	37	40	38	9.59E+02
95.8	0.99	2.4	49	42	45	1.01E+03

III.1.B. Plot of Energy vs Count for $^{22}_{11}\text{Na}$ Source

Figure 4 :: β -ray spectrum of $^{22}_{11}\text{Na}$

III.1.C. Energy corresponding to the maximum count for $^{22}_{11}\text{Na}$ source

The peak of the spectrum was observed to be at an energy of 310.36 keV with the average count of 134.

III.2. $^{90}_{38}\text{Sr}$ Source

For the $^{90}_{38}\text{Sr}$ source, we decided to take only one run for each voltage, again, for 60 seconds. However, this time the voltage was varied at a slower rate compared to that of the $^{22}_{11}\text{Na}$ source, to make sure we have more close-by datapoints to get a better and more accurate spectrum.

III.2.A. Table for $^{90}_{38}\text{Sr}$ Source

Magnetic Field(mT)	Voltage (V)	Current (A)	Counts	Corrected Counts (no background)	Energy (keV)
0	0	0	109	0	0.00E+00
4.6	0.06	0.1	216	107	4.63E+00
5.6	0.08	0.2	230	121	6.85E+00
7	0.1	0.2	256	147	1.07E+01
7.9	0.12	0.3	280	171	1.36E+01
9.4	0.14	0.3	301	192	1.91E+01
10.8	0.16	0.4	329	220	2.50E+01
12.2	0.18	0.4	327	218	3.18E+01

14.2	0.2	0.4	351	242	4.26E+01
15.1	0.22	0.5	398	289	4.79E+01
16.7	0.24	0.5	444	335	5.81E+01
17.9	0.26	0.6	428	319	6.62E+01
19	0.28	0.6	471	362	7.41E+01
20.6	0.3	0.7	488	379	8.61E+01
22.4	0.32	0.7	563	454	1.01E+02
24.6	0.34	0.8	609	500	1.19E+02
25.2	0.36	0.8	643	534	1.25E+02
27.3	0.38	0.9	666	557	1.44E+02
28.6	0.4	0.9	698	589	1.56E+02
30.7	0.42	1	772	663	1.77E+02
31.9	0.44	1	796	687	1.89E+02
33.6	0.46	1.1	826	717	2.07E+02
34.6	0.48	1.1	830	721	2.17E+02
36.7	0.5	1.2	951	842	2.40E+02
38.5	0.52	1.2	1034	925	2.60E+02
39.6	0.54	1.3	975	866	2.72E+02
41.9	0.56	1.3	1126	1017	2.99E+02
43.3	0.58	1.3	1126	1017	3.15E+02
45.4	0.6	1.4	1118	1009	3.40E+02
46.7	0.62	1.4	1256	1147	3.56E+02
48.4	0.64	1.5	1235	1126	3.77E+02
51.2	0.68	1.6	1353	1244	4.11E+02
54.7	0.72	1.7	1389	1280	4.55E+02
59	0.76	1.8	1480	1371	5.11E+02
62.2	0.8	1.9	1500	1391	5.52E+02
65.3	0.84	1.9	1545	1436	5.93E+02
70.5	0.9	2.1	1580	1471	6.63E+02
75.6	0.96	2.2	1547	1438	7.32E+02
81.2	1.02	2.4	1528	1419	8.09E+02
87.8	1.08	2.5	1494	1385	9.01E+02
92.2	1.14	2.7	1530	1421	9.63E+02
98.1	1.2	2.8	1414	1305	1.05E+03
102.2	1.26	2.9	1373	1264	1.10E+03
107.7	1.32	3.1	1265	1156	1.18E+03
113.3	1.38	3.3	1138	1029	1.26E+03
118.1	1.45	3.4	1081	972	1.33E+03
123.4	1.5	3.5	962	853	1.41E+03

128	1.56	3.7	869	760	1.47E+03
132.5	1.62	3.8	781	672	1.54E+03
137	1.68	4	748	639	1.61E+03
142.4	1.74	4.2	744	635	1.68E+03
149.1	1.8	4.3	561	452	1.78E+03
151.3	1.86	4.5	508	399	1.81E+03
155.9	1.92	4.6	508	399	1.88E+03
161.3	2	4.8	398	289	1.96E+03

III.2.B. Plot of Energy vs Count for $^{90}_{38}\text{Sr}$ Source

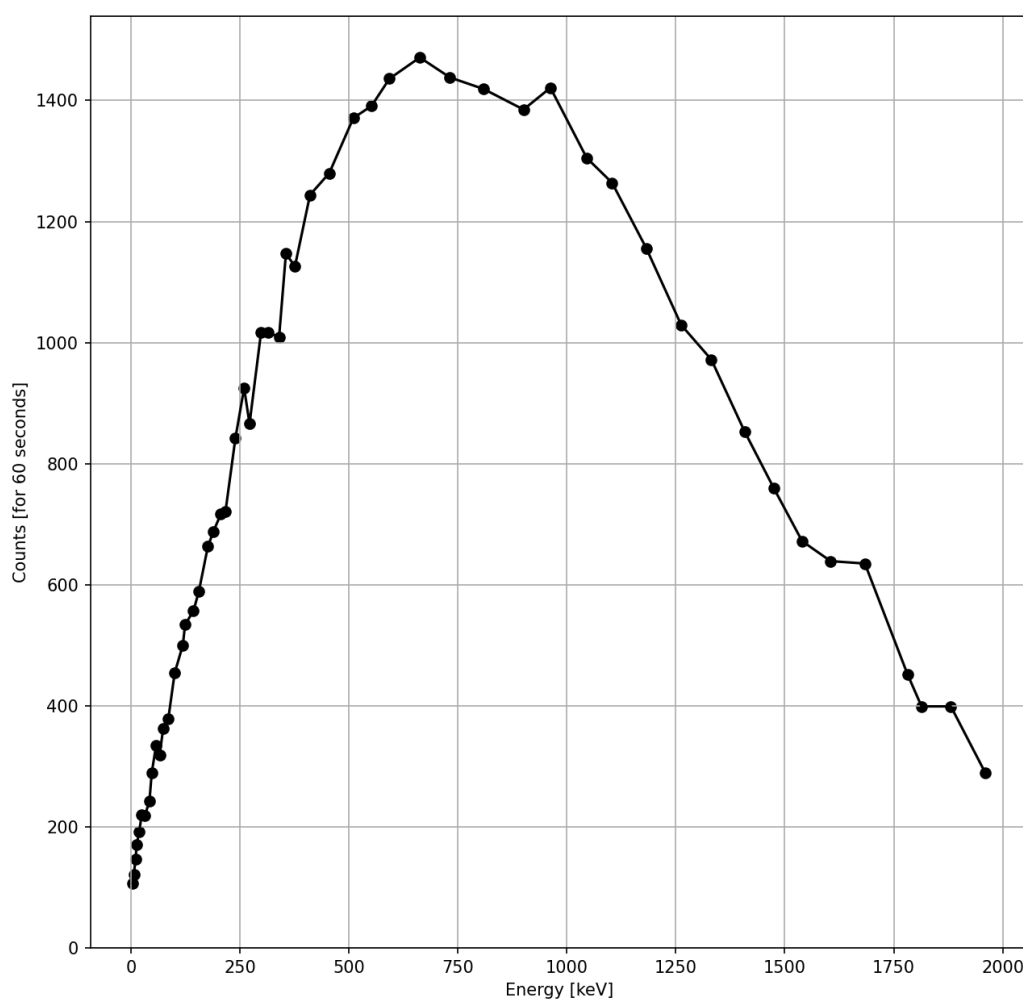


Figure 5 :: β -ray spectrum of $^{90}_{38}\text{Sr}$

III.2.C. Energy corresponding to the maximum count for $^{90}_{38}\text{Sr}$ source

The peak of the spectrum was observed to be at an energy of 662.83 keV with the average count of 1471.

IV. Sources of Error

1. A primary source of error is the comparatively high dead time of a Geiger-Mueller counter. This is a greater source of error for the Strontium source, due to the higher count rate. Any β radiation that is incident on the GM counter during the dead time will not trigger a series of Townsend avalanches and will not be registered as a count.
2. The efficiency of response of the GM counter is also a function of the energy of the incident radiation, and this introduces a systematic error into the spectrum that is being recorded.
3. Non-uniformity in the magnetic field created by passing current through the conducting coil can cause errors. Since the region where the β radiation is being emitted and captured lie outside of the solenoid, the field is not uniform. We have not accounted for the edge corrections in the magnetic field near the ends of a finite length solenoid, and thus these errors are present in the spectra that we have recorded.
4. Electrical fluctuations that might affect the counting equipment and the power sources used in the experiment are a source of error.
5. The β radiation particles also undergo some amount of energy straggling as they travel from the source to the GM counter, as the space between them is not an evacuated vacuum. It is reasonable to expect different β particles to have undergone different histories and thus have lost differing amounts of energy in the space between the detector and the source. This causes the spectra readings to be more diffuse than they ideally should be.
6. The assumption that the entire conical solid angle in which the radiation source puts out β particles has the same number density of the particles is erroneous, as we have not accounted for geometric factors such as the positioning of the radioactive material in the source. If the number density of β particles at some angle from the center of the cone (measured over a long enough period of time) changes as a function off the angle, this would introduce errors into the spectra that we have measured.

V. Conclusion

In this experiment we succesfully recorded the β -ray spectra for $^{22}_{11}\text{Na}$ and $^{90}_{38}\text{Sr}$, using a β -ray spectrometer, and obtained the peak emission energy for both.